Development of a Large Inert Gas Ion Thruster

G. Steiner*
Xerox Electro-Optical Systems, Pasadena, California

A 30-cm inert gas electrostatic ion thruster exhibiting excellent performance has been developed. In the development, the effective anode area was reduced by altering the magnetic field geometry to improve plasma containment, consistent with operational stability. The propellant introduction scheme has the effect of "folding" the discharge chamber without the increased wall loss penalty associated with a longer chamber. These features contribute to a low discharge cost (eV/ion) vs mass utilization characteristic which remains relatively flat even to high mass utilizations.

Introduction

FUTURE stationkeeping needs of large space systems virtually dictate the use of electric propulsion.[1,2] Environmental and spacecraft contamination considerations make the use of noncondensing inert gases highly desirable as propellants. Additional advances in mass and electrical efficiencies serve to widen the already significant gap for this application between electric and chemical propulsion technologies of required propellant storage mass. Thruster size is determined by thrust requirements. A 12-cm (diameter of active electrode area) inert gas thruster has been extensively investigated.[3] The development of the next size, 30 cm, to operate on either argon or xenon propellant is reviewed here. The design and performance optimization process is presented, with emphasis on the scalability of the former as other thrust requirements are identified.

Size Selection

A previously published study[4] identified the optimum size for a large inert gas ion thruster. Basically, specification of a maximum thrust level defined a thruster diameter. An upper bound was placed on this diameter by practical constraints such as electrode technology. 50 cm was identified as an optimal compromise between argon and xenon propellants for the maximum diameter of a range of thruster sizes. Invoke further practical contraints such as the availability of a ground vacuum test facility and proven electrode technology, and 30 cm emerges as a logical choice for the diameter of an intermediate developmental thruster.

Discharge chamber length is chosen to provide efficient ionization with a minimum multiple-charged ion production rate. The plasma containment scheme and mode of propellant introduction also influence these parameters. Because of this and dual specie operation, length was left as an experimental variable to be optimized empirically. Basic chamber length was based on a prediction of the xenon optimum and cylindrical extensions were used for argon optimization. With a diameter and minimum length defined, the prolate hemispheriod discharge chamber shape was chosen to provide a large active ion production volume to wall loss surface area ratio.

Presented as Paper 82-1927 at the AIAA/JSASS/DGLR 16th International Electric Propulsion Conference, New Orleans, La., Nov. 17-19, 1982; received Dec. 13, 1982; revision received April 9, 1984.

*Physicist.

Length Investigation

Rapid evaluation of various discharge chamber lengths was accomplished with one or more bolt-on chamber extensions. Lengthening the chamber was expected to improve mass utilization by increasing the path an atom must travel before escaping as a neutral, thus increasing the probability of ionization but at the same time increasing wall losses. The test results of Figs. 1 and 2 support these hypothesis. Dashed portions of the curves indicate extrapolations based on argon-xenon correlation and 12-cm thruster data.[3]

Further optimization of the plasma containment configuration with longer chamber lengths could somewhat counteract the upturn in the discharge cost of Fig. 2, but the gain in mass utilization by operating at this length would be very small. A better operating point exists just above the knee of the mass utilization curve (Fig. 1) where the discharge cost and thruster size are small. 15 cm was identified as the optimum length for further investigation of other discharge chamber parameters.

Propellant Introduction

Prime objectives in the introduction of the propellant into the discharge chamber were maximization of the chance of ionization before neutral atoms escaped through the ion optics set and minimization of the rate of multiple ion production. Plasma density uniformity across the electrode plane to operate each aperture near its perveance limit requires that propellant introduction not induce pronounced neutral density gradients in this region.

Three propellant introduction schemes were investigated as illustrated schematically in Fig. 3. The first configuration tested has three nozzles around the cathode directed downstream and coaxially with the thruster axis. A variation of this, with the nozzles located midchamber and directed radially inward, gave slight improvements in plasma density and its uniformity across the electrode plane.

To improve mass utilization, neutral atoms must remain in the chamber longer to increase the probability of an ionizing collision before escape through the electrodes. A simple way to increase the residence time is to lengthen the chamber, but this incurs an increased wall loss penalty. Injecting the propellant at the electrode plane around the periphery and directing it upstream folds the path neutrals must take to escape by bouncing them off the upstream chamber walls. This more than doubles the average residence time without the increased wall loss penalty of lengthening the chamber. This technique of reverse-directed main propellant introduction was used exclusively in the performance mapping of the thruster reported in the final section and demonstrated high mass utilizations with a very short discharge chamber.

Plasma Containment

Several containment schemes were employed, but all were characterized by an intense multiple ring cusp magnetic field using a hollow cathode as the electron source. The natural extension from the previous 12-cm size[3] was simply to continue this optimized Magneto-Electrostatic Containment (MESC) anode/magnet spacing to cover the interior of the 30-cm chamber as illustrated in Fig. 4. Adjusting the anodes to the proper magnetic field immersion for this configuration produced performance exceeding that expected from simple volume-to-surface area improvements over the 12-cm version. This can be attributed to discharge chamber dimensions now comparable to the mean free path for ionization, in contrast to the several bounces required on average for ionization in the smaller chamber. This improves ion generation when the ionization cross section is fixed and the ratio of propellant throughout to electrode open area is the same for both thrusters.

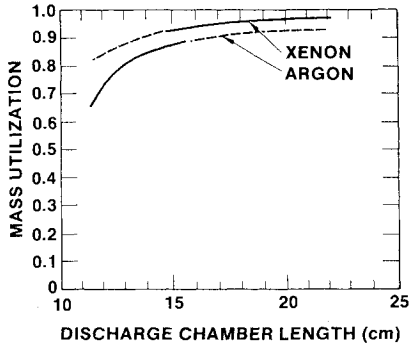

Fig. 1 Discharge chamber length investigation, effect on maximum achieved mass utilization.

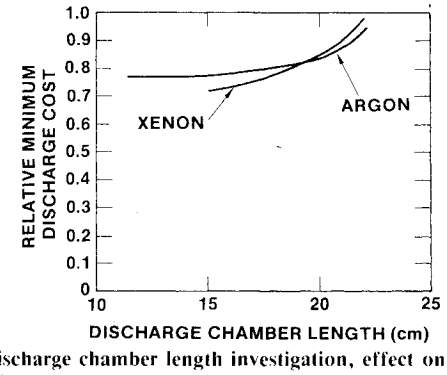

Fig. 2 Discharge chamber length investigation, effect on minimum achieved discharge cost.

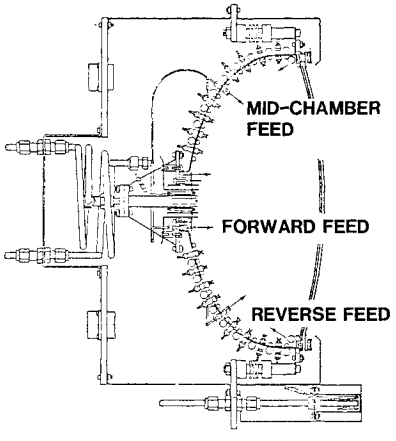

Fig. 3 Propellant introduction schemes.

Sovey[5] reported an improvement in performance with his line cusp thruster when electrically isolated anodes were removed and the discharge chamber and magnets were tied to anode potential. A similar effort reported by Ramsey[3] with the 12-cm line cusp MESC thruster also exhibited a reduction in discharge cost (eV/ion) when the anode strips were omitted and the magnetic circuit assembly served as a "shell anode." This prompted the analogous experiment with the traditional ring cusp (magnet rings coaxial with the thruster axis) MESC 30-cm thruster. The electron bombardment heating of magnets and possible thermal de-Gaussing was of major concern, however. This shell anode verions of the ring cusp MESC thruster has essentially only the magnet faces to serve as concentrated anode areas, in contrast to the preious tantalum strip anodes thermally isolated from the magnets. A precautionary step was taken to minimize the risk of magnet thermal damage. Experience with occasional magnet damage in the past indicated that highly localized discharge current attachment and the resulting concentrated heating was the destructive mechanism. This phenomenon was encountered during the high-pressure discharge mode immediately following the propellant flooding technique of thruster startup. To dissipate this energy over a large area, a copper liner was installed over the magnets for good heat conduction and minimum perturbation of magnetic field. This configuration was termed "monoanode" because of the cooper liner serving a single anode surface as shown in Fig. 5.

A further mechanical simplification was made on the basis of the absence of any evidence of magnet overheating. This simply amounted to the removal of the monoanode copper liner, allowing the discharge current to attach directly to the magnet faces. Further testing produced no evidence of

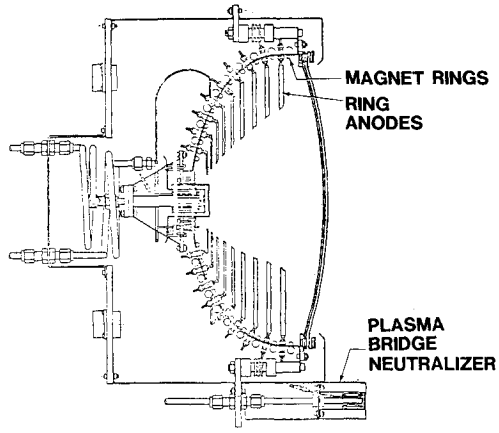

Fig. 4 30-cm inert gas laboratory MESC ion thruster schematic.

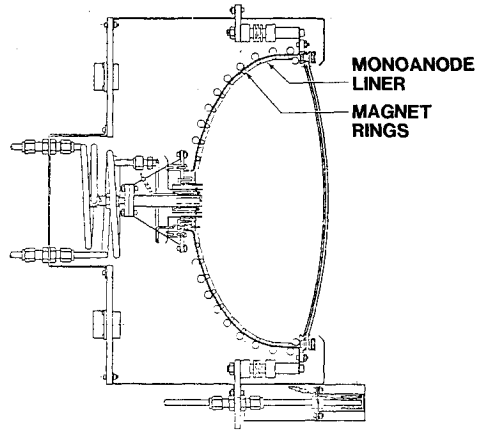

Fig. 5 30-cm monoanode inert gas ion thruster.

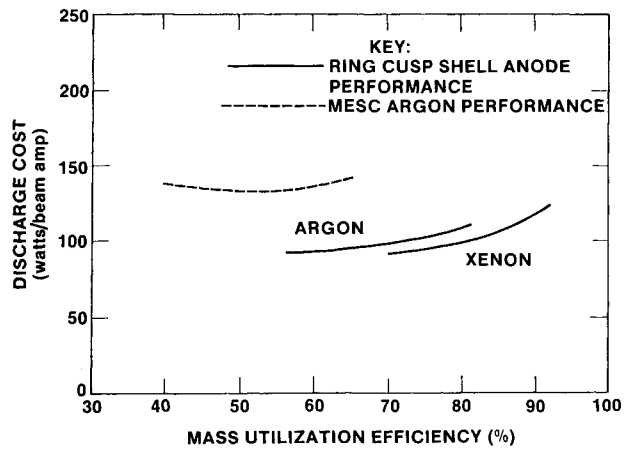

Fig. 6 Discharge cost vs mass utilization performance (corrected for double ion beam content and neutral ingestion).

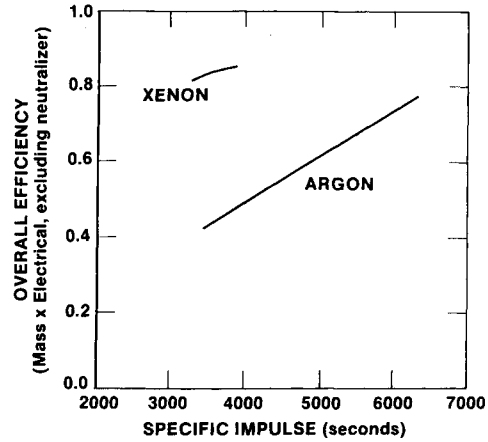

Fig. 8 Ring cusp shell anode, overall efficiency vs specific impulse (corrected for double charged ion beam content and neutral ingestion).

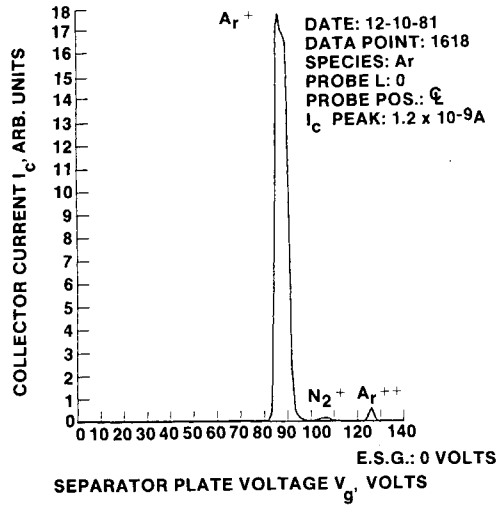

Fig. 7 E×B mass spectrometer ion beam analysis.

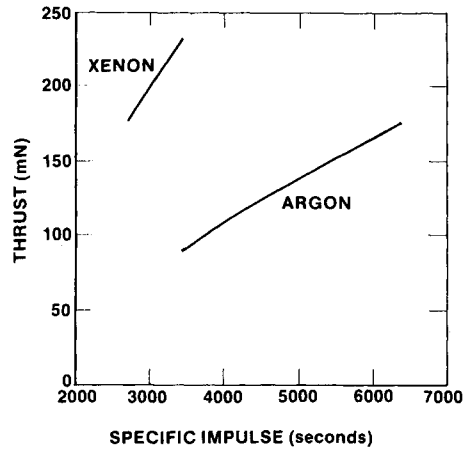

Fig. 9 Ring cusp shell anode, thrust vs specific impulse (corrected for beam divergence, double charged ion beam content, and neutral ingestion).

damage, so the copper liner was deemed unnecessary, at least for this level of developmental testing.

Kaufman et al.[6] identified anode area as an important factor governing performance. Reductions in effective anode area generally precipitated improved performance. With the traditional MESC concept this was accomplished by lowering the strip anodes into higher magnetic field regions. With the strip anodes removed, leaving a ring cusp shell anode configuration, anode area reduction was effected by, increasing magnet ring pitch and supplementing the magnetic field intensity to maintain intercusp field intensity. Discharge chamber optimization generally encompassed successive effective anode area reductions and identification of loss mechanisms, consistent with operational stability.

Performance Results

Initial discharge chamber optimization was accomplished with several discharge mode diagnostic techniques. These included Langmuir probes, measurements of plasma radiation, and a biased accel grid as proposed by Sovey.[5] The latter is essentially a large Langmuir probe to measure the ion saturation current over the electrode region. Final assessment of performance relied ultimately on actual beam extraction testing. A hollow cathode neutralizer was used for all beam extraction testing. Some limited three grid ion optics data were gathered, but the majority of the testing used a two grid set.

Test results of the MESC version of the minimum length thruster were reported previously in detail[4] but are shown as a dashed line in Fig. 6.

All remaining test results pertain to the optimized ring cusp shell anode thruster. Corrections for double charged ion beam content were based on E×B mass spectrometer data in a manner described by Vahrenkamp.[7] As a conservative measure, worst case on-axis E×B mass spectrometer data such as those shown in Fig. 7 was applied for the correction of performance figures. This instrument was also able to resolve residual gas (N_2^+ peak) in the discharge chamber. All data presented in Fig. 6 and 8-10 included both the multiple charged ion and neutral atom ingestion corrections. The latter is a linear function of vacuum chamber pressure and electrode open area.

The low discharge cost vs mass utilization curve of Fig. 6, which remains relatively flat even to high mass utilizations, is attributed to the reverse main feed propellant introduction scheme. For comparison, the performance achieved with MESC version is shown as a dashed curve and graphically illustrates the improvement in performance gained with ring cusp shell anode/reverse feed thruster.

In Fig. 8, high efficiency over the entire specific impulse range is desirable, but the thruster was not performance mapped in this manner. Rather, discharge chamber performance was emphasized with little variation in specific impulse attempted, except that influenced by the mass utilization. The same is true of Fig. 9. Specific impulse is

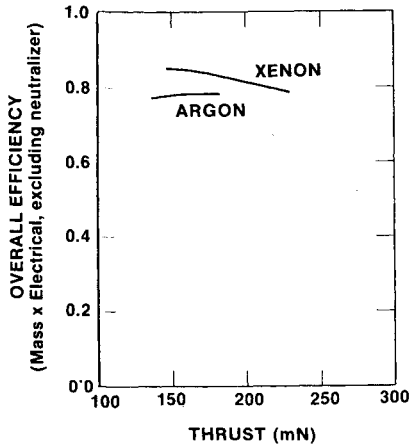

Fig. 10 Ring cusp shell anode, overall efficiency vs thrust (corrected for beam divergence, double charged ion beam content, and neutral ingestion).

generally an ion optic phenomenon except for the dependence on mass utilization. But ion optics was not extensively investigated in this discharge chamber optimization. This is apparent in the relatively narrow range of operation in Fig. 8 and 9, but these are not to be construed as indicative of thruster limitations. Plotted results only typify the operating points used in this experiment.

A plot which better characterizes the high level of performance achieved within this range of operating is shown in Fig. 10. Overall efficiency remains high over the thrust levels tested, but again only limited throttle data were gathered. Similar levels of performance are considered achievable as a function of specific impulse (Fig. 8) as the net accelerating potential is varied within the lower and upper bounds of the onset of space charge limitation and electrical breakdown, respectively.

Conclusion

A 30-cm inert gas ion thruster was developed, exhibiting outstanding performance. Argon discharge cost minimum was a record low 91 watts per beam amp (corrected) and xenon extrapolated to a 80 watt/beam amp minimum. At 80 and 92% mass utilization, these figures rose to only 111 and 126 watts/beams amp, respectively. The nature of the plasma containment scheme with its mechanical simplicity lends itself well to scaling to other thruster sizes as different thrust requirement emerge.

Acknowledgment

This work was supported by the NASA Lewis Research Center under contract NAS3-22444.

References

[1] "Large Space Systems/Low Thrust Propulsion Technology," NASA Conference Publication 2144, May 1980.

[2] "Large Space Systems/Propulsion Interactions," NASA Technical Memorandum 82904.

[3] Ramsey, W. D., "Inert Gas Tests of Two 12-cm Magneto-Static Thrusters," AIAA Paper 82-1925, Nov. 1982.

[4] Ramsey, E. J., Steiner, W., and Steiner, G., "Developing a Scalable Inert Gas Ion Thruster," AIAA Paper 82-1275, June 1982.

[5] Sovey, J. S., "Performance of a Magnetic Multipole Line-Cusp Argon Ion Thruster," AIAA/JSASS/DGLR 15th International Electric Propulsion Conference, Las Vegas, Nev., April 1981, and NASA Technical Memorandum.

[6] Kaufman, H. R., and Robinson, R. S., "Inert Gas Thrusters," NASA CR159813, Nov. 1979.

[7] Vahrenkamp, R. P., "Measurement of Double Charged Ions in the Beam of a 30-cm Mercury Bombardment Thruster," AIAA 10th Electric Propulsion Conference, Lake Tahoe, Nev., Oct. 1973.